# Modeling Ebola: Three Distinct Models with Similar Predictions

Hsuan-Wei Lee[1], Anzhelika Lyubenko[2], Yuhang Ma[3], Emily Meissen[4], Daniela Velez-Rendon[5], Nara Yoon[6]

Mentors: John Peach [7], Cammey Cole Manning[8], Christian Gunning[9]

**Abstract**

We present and compare three models of the Ebola outbreak in Liberia during 2014-2015 and examine the effect of international intervention. We utilize both system dynamics and agent-based approaches. We show that the basic reproduction number of the disease is greater than one before intervention and decreases to less than one after intervention, implying eventual eradication of the disease. We demonstrate that the probability of an outbreak varies depending on the population size and that even for large populations there is a 70% chance of an outbreak if only one person gets exposed to the disease. In addition, if an outbreak is not contained in the early stages and the individuals do not change their behavior as the virus prevails, over 90% of population contract the disease and about 50% of the population dies because of it. Effective intervention may decrease both figures to be less than 1%. When including spatial movement in the agent-based setting, we conclude that outbreaks can be less severe due to the population not being well-mixed, the spread between community members is the highest proportion of transmission, and that the common practice of touching the deceased at a funeral accounts for a significant portion of disease contractions (13% in the model).

# 1 Introduction

The massive outbreak of Ebola in Africa in the past two years has generated interest in modeling the spread of disease for the purpose of predicting such outbreaks and determining how to prevent them in the future. In this paper, we focus on the spread of Ebola through Liberia in 2014-2015, due to the availability of relevant data for cases of Ebola infections in Liberia in the literature. Using properly calibrated parameters, our models can be used to consider other countries or diseases to predict and prevent outbreaks.

Ebola was first discovered in 1976. Between 1976 and 2014, there were 34 recorded occurrences of Ebola reported by the Centers for Disease Control and Prevention. Until 2014, only small outbreaks occurred, with less than 500 reported deaths per outbreak – 11 such outbreaks had less than 10 recorded deaths, and 15 outbreaks had less than 65 deaths [4]. In contrast, the 2014 outbreak has taken thousands of lives over the past two years and has received extensive media coverage.

Earlier outbreaks of Ebola were contracted in Central Africa, where it was first discovered, but the current outbreak took place in West Africa. The early symptoms are flu-like – fever, headache, fatigue, and joint pain – which may have initially masked the identity of the virus, because other common diseases to the area, such as HIV and Malaria, share these symptoms. As the Ebola virus progresses through an individual, he experiences abdominal pain, diarrhea, vomiting, and rashes. The virus is contracted through direct contact with bodily fluids (e.g. blood, saliva, urine, fecal matter) and physical objects contaminated by such fluids, and once the virus is contracted, the incubation period may last up to two weeks making tracking difficult [2]. A variety of cultural and economic factors has also contributed to the spread of the disease: lack of medical centers and poor sanitation practices in such centers, distrust of western medicine, poverty of local governments and individuals, and physical contact with the deceased in traditional burial ceremonies[10].

We model the spread of Ebola with both system-based and agent-based models. In the system-based model, the population is divided into compartments (or states). As time progresses, people flow from one compartment into another. These dynamics are described by differential equations. One of the most well-known system-based models is the SIR model which involves three states: susceptible (S), infected (I) and

[1]Department of Mathematics, University of North Carolina Chapel Hill
[2]Department of Mathematical and Statistical Sciences, University of Colorado Denver
[3]Department of Operations Research and Information Engineering, Cornell University
[4]Program of Applied Mathematics, University of Arizona
[5]Department of Bio-engineering, University of Illinois at Chicago
[6]Department of Mathematics, Applied Mathematics and Statistics, Case Western Reserve University
[7]Massachusetts Institute of Technology: Lincoln Laboratory
[8]Department of Mathematics and Computer Science, Meredith College
[9]Departments of Entomology and Mathematics, North Carolina State University

recovered (R). From this, other models are generated with more compartments. In the case of Ebola, Lekone and Finkenstd [7] consider a four-compartment model, inserting an "exposed" state between the susceptible and infected states. A six-compartment model, presented by Legrand [6] and Rivers [12], differentiates between the disease spread rates in the community, at hospitals and medical centers, and at funerals.

In contrast to system-based models, agent-based models are concerned with the behavior of a typical individual and probabilistic events rather than the deterministic behavior of the overall system. In such models, each individual has a state and the individual transitions to other states probabilistically at each time step. Agent-based models for Ebola in the previous literature include Siettos et al. [13] and Merler et al.[8]. A variety of models examine the effectiveness of intervention measures, including contact tracing by Webb et al. [14] and incorporating travel restrictions by Poletto et al. [11].

This paper presents a seven-compartment model, used in both the system and agent-based dynamics. We show that an intervention can cause the trajectory of the spread of the disease to change significantly. The deterministic model predicts that over 50% of the population who would have died from the disease never contract it due to intervention. The probabilistic model also reveals similar results.

In Section 2 we present the seven-compartment model and discuss assumptions and parameters used throughout the paper. Section 3 presents the system-based model and calibrates parameters used for the rest of the paper. Sections 4 and 5 present agent-based models, the former based on the flows of the system-based model and the latter incorporating spatial movement of individuals. In Section 6 we summarize the results and discuss future extensions of the models and approaches.

# 2 Methods

The system-based and agent-based models use the same seven classes and transitions. Here we present the seven-compartment model as well as the shared assumptions and parameters between the models.

## 2.1 Compartment-State Definition

Based on the model and parameters published by Rivers et al.[12], this model divides the population into seven compartments: susceptible (S), exposed (E), infected (I), recovered (R), hospitalized (H), funeralized (F), and dead (D) individuals. The permissible transitions are as pictured in Figure 1. Susceptible individuals may become exposed if they come into contact with an infected individual, initiating a transition to the infected state after the incubation period of the disease. Once infected, individuals acquire the capacity to infect others. Some infected individuals may be hospitalized. There are two possible outcomes for the unhospitalized infected individuals and the hospitalized individuals: they may die, with a probability of infecting other people during the resulting funeral, after which they are buried and no longer affect others, or they may recover. Employing separate states for recovered and dead individuals, although both are removed from affecting the future dynamics of the disease, allows the tracking of the severity of disease.

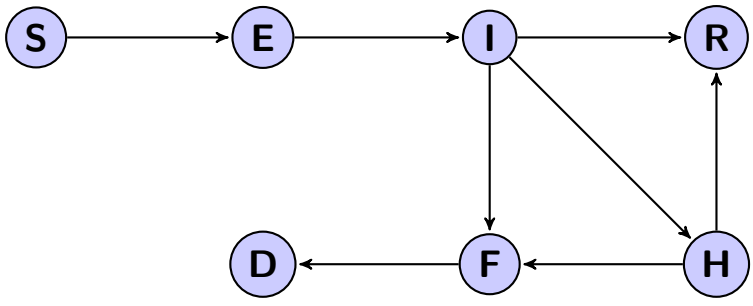


Figure 1: The seven-compartment model of susceptible (S), exposed (E), infected (I), recovered (R), hospitalized (H), funeralized (F), and dead (D) individuals. Flows or probabilistic transitions of individuals are allowed between states as indicated by arrows.

### 2.2 Assumptions and Parameters

We assume that no births or deaths occur during the modeled time period, other than the deaths related to Ebola. The relevant parameters are listed in Table 1 and Table 3, with the latter calibrated for Liberia.

| Parameter | Value | Reference |
|---|---|---|
| Incubation Period ($t_P$) | 11 days | [9] |
| Duration of Traditional Funeral ($t_F$) | 2 days | [12] |
| Time of Infection to Recovery ($t_I$) | 10 days | [12] |
| Time from Infection to Death ($t_D$) | 8 days | [12] |
| Case Fatality Rate, Unhospitalized ($\delta_1$) | 0.5 | [9] |
| Case Fatality Rate, Hospitalized ($\delta_2$) | 0.5 | [9] |

Table 1: Model Parameters for Ebola Epidemic in Liberia with literature citations.

## 3 System Dynamics

We use a system of differential equations to model the dynamics between the states listed in Section 2.1. The diagram of the described compartment model, with compartments and flows, is depicted on Figure 2.

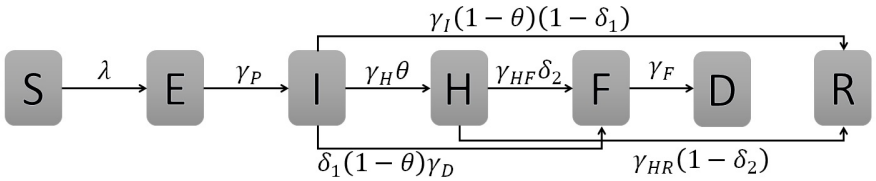


Figure 2: The compartment model from Section 2.1 with flow parameters. All possible flows are specified by the arrows and parameters.

The governing equations of the system dynamics shown above are the following:

$$\frac{dS}{dt} = -\frac{\beta_I SI + \beta_H SH + \beta_F SF}{N} \tag{1}$$

$$\frac{dE}{dt} = \frac{\beta_I SI + \beta_H SH + \beta_F SF}{N} - \gamma_P E \tag{2}$$

$$\frac{dI}{dt} = \gamma_P E - [\gamma_H \theta + \gamma_I(1-\theta)(1-\delta_1) + \gamma_D(1-\theta)\delta_1]I \tag{3}$$

$$\frac{dH}{dt} = \gamma_H \theta I - [\gamma_{HD}\delta_2 + \gamma_{HR}(1-\delta_2)]H \tag{4}$$

$$\frac{dF}{dt} = \gamma_D(1-\theta)\delta_1 I + \gamma_{HD}\delta_2 H - \gamma_F F \tag{5}$$

$$\frac{dR}{dt} = \gamma_I(1-\theta)(1-\delta_1)I + \gamma_{HR}(1-\delta_2)H \tag{6}$$

$$\frac{dD}{dt} = \gamma_F F \tag{7}$$

The $\gamma$ terms refer to the reciprocal of their respective time periods. The interpretations of $t_P, t_F, t_I$, and $t_D$ can be found in Table 1; $t_H$ refers to the time from infection to hospitalization; and $t_{HD}$ and $t_{HR}$ refer to the time from hospitalization to death and recovery, respectively. The case fatality rates, $\delta_1$ for unhospitalized individuals and $\delta_2$ for hospitalized individuals, are found in Table 1, and $\theta$ refers to the probability that a case is hospitalized. The effective contact rates, $\beta_I, \beta_H, \beta_F$, are the numbers of infections resulting from the $I, H, F$ compartments per unit time. Here $SI/N$, $SH/N$, and $SF/N$ represent the number of possible contacts between the susceptible compartment and the infected, hospitalized, and funeralized compartments,

and hence multiply the contact rates in Equations 1 and 2. In Figure 2, we define $\lambda = (\beta_I I + \beta_H H + \beta_F F)/N$, a combination of the $\beta$ contact rates shown in Table 1 and 3.

The equations described obey total conservation, guaranteeing that the total of the compartment values remains constant. This can be seen by adding all terms on the right-hand sides, which sum to 0. The transmission rate $\beta$ is the parameter representing all the complexity in the transmission process like contact frequency, infection probability per contact and so on. $\theta$ refers to the probability of a case being Hospitalized and $\delta$ to the case fatality rate (See Tables 1 and 3).

Equation 1 describes the change with respect to time of the susceptible population. The transition from S to E depends on $\beta_I SI + \beta_H SH + \beta_F SF$, which is the contact rate with the compartments I, H and F (all of which are infectious), and the respective number of value of each compartment.

Equation 2 describes the change in the exposed compartment. This depends on the flow leaving S and the flow from E to I normalized by the incubation period $t_P$.

Equation 3 describes the change in the infected compartment, which adds the flow from E. Flows out of compartment I include the flow from I to H, which is given by the product between the transition rate from I to H and the probability of hospitalization hospitalized; in the same way, subtracting the individuals that transitions from I to R, given by the product among the duration of infection rate, the probability a case is not hospitalized and the death rate of an unhospitalized case. Finally substracting the individuals that transitions from I to F , given by the product between the transition rate from Infected to Dead, the probability a case is NOT hospitalized and the death rate of an unhospitalized case.

Equation 4 describes the changes in the hospitalized patients. It depends on the number of individuals that transition from I to H, given by the product between the transition rate from infected to hospitalized and the probability a case is hospitalized; substracting the individuals than transitions from H to D, given by the product among the transition rate from hospitalized to Dead and the death rate of a hospitalized case, and finally, susbtracting the people that transitions from H to R, which is given by the product between the transition rate from I to R and the survival rate of an hospitalized case.

Equation 5 describes the changes in the funeralized compartment. Depending on the number of individuals that transitions from I to D, which is given by the product between the transition rate from I to D, the probability a case is not hospitalized and the death rate of an unhospitalized case. Adding the people who transitions from H to F , which is given by the product between the transition rate from H to D and the death rate of an hospitalized case. Finally substracting the individuals who already have been buried.

Equation 6 describes the changes in the recovered compartment. Depending on the transition from I to R, which is given by the product between the duration of infection rate, the probability a case is not hospitalized and the survival rate of an unhospitalized rate. Adding the individuals who transitions from H to I, which is given by the product among the transition rate from I to H and the survival rate of a hospitalized case.

Equation 7 describes the changes on the dead compartment, which solely depends on the rate of duration of a traditional funeral.

### 3.1 Parameter Calibration

The parameter values which represent biological processes ($\alpha, \gamma_I, \gamma_D, \delta_1, \delta_2$) or social customs ($\gamma_F$) had values listed in the previous literature [11, 14], while the parameters which represent social behavior ($\mathcal{P} = \{\beta_I, \beta_H, \beta_F, \gamma_H, \theta\}$) depend on infection region (see Tables 1 and 3 and Equations 1 to 7 for the parameter definitions). The parameters $\gamma_{DH}$ and $\gamma_{IH}$ are also unknown, but we assume the following relation with known parameters: $1/\gamma_{DH}=1/\gamma_D$-$1/\gamma_H$ and $1/\gamma_{IH}=1/\gamma_I$-$1/\gamma_H$. Here, we calibrate $\mathcal{P}$ based on our systematic model (Equations 1-7) and the data of cumulative deaths in Liberia from March 2014 to July 2015 from World Health Organization (WHO) [3].

### 3.2 Bayesian Calibration Framework

We use Bayesian methodology to calibrate the unknown system parameters. This method is utilized in many calibrations of complicated systems owing to its merit that little or no information of the parameter values is needed for its usage. The calibration procedure starts from choosing a distribution in the space of parameters. This distribution, the "prior distribution" ($\mathcal{D}_0$), can be a simple distribution such as uniform or other intuitively chosen parametric distribution. Based on the available data and mathematical setup, we

evaluate the likelihood weight for the samples from $\mathcal{D}_0$ with which we update the "posterior distribution" ($\mathcal{D}_1$). Multiple updates ($\mathcal{D}_1$ to $\mathcal{D}_2$, $\mathcal{D}_2$ to $\mathcal{D}_3$, ...) facilitate a more accurate distribution.

To calibrate the unknown parameters ($\mathcal{P}$), we started from an uniform prior distribution in the range determined based on numerical exploration and other papers (see Table 2) [12].

| $\beta_I$ | $\beta_H$ | $\beta_F$ | $\gamma_H$ | $\theta$ |
|---|---|---|---|---|
| $(0, 0.5)$ | $(0, 0.5)$ | $(0, 1)$ | $(2, 7)$ | $(0, 0.5)$ |

Table 2: Range of the prior parameter space

To each random choice ($\mathcal{P}_0$) from the prior distribution, we assigned a likelihood weight by comparing the World Health Organization (WHO) data reports ($\mathcal{D}_R$) to the data simulated with $\mathcal{P}_0$ ($\mathcal{D}_S$) from the systems-based model. Repeating this method, we build the posterior distribution for $\mathcal{P}$. In this methodology, we provide multiple likely parameter sets, rather than a single best fit, by listing the mean as well as the standard deviation of suggested parameter values. The algorithm for the parameter calibration is:

Step 1) Choose a random $\mathcal{P}_0$ from the prior distribution.

Step 2) Solve the deterministic system (Equations 1-7) with $\mathcal{P}_0$ and given initial value $\{S_0, E_0, I_0, H_0, D_0, R_0\}$, then evaluate $\mathcal{D}_S = \{D(t_i)\}$ for all dates $\{t_i\}$ corresponding to the cumulative death data ($\mathcal{D}_R$).

Step 3) Evaluate likelihood of $\mathcal{P}_0$: $\exp\left(-\|\mathcal{D}_R - \mathcal{D}_S\|_2/\|\mathcal{D}_R\|_2\right)$.

*Repeat Steps 1-3 many times to generate parameter and likelihood estimates. Generate the posterior distribution using these weights.*

### 3.2.1 Results and validation

We applied our systematic model and calibration method to the Ebola spread in Liberia during 2014-2015. Two sets of cumulative mortality data (pre-intervention and post-intervention) were used to calibrate pre- and post-intervention parameters, respectively. We assume that about a fourth (1 million) of Liberia's total population (4.3 million [1]) are involved in the model, and that the rest of the population do not have any chance of acquiring the disease due to geographical location or behavioral reasons. For the calibration of pre-intervention parameters, we used the data from 176 days (March 2014 to September 2014) and initial values $\{S_0, E_0, I_0, F_0, D_0, R_0\}$=$\{10^6 - 1, 0, 1, 0, 0, 0\}$ assuming that the initial outbreak started from a single infected person. The calibration of post-intervention parameters is based on the data from 306 days (September 14 to July 15) and initial values $\{S[176], E[176], I[176], F[176], D[176], R[176]\}$ which are evaluated from the calibrated parameter means $\mathcal{P}$ for pre-intervention. Each calibration used 10,000 random samples.

| Parameter | Pre-Intervention (Mar 2014 to Sept 2014) | Post-Intervention (Sept 2014 to July 2015) |
|---|---|---|
| Contact Rate, Community ($\beta_I$) | 0.148 (0.0953) | 0.0446 (0.0338) |
| Contact Rate, Hospital ($\beta_H$) | 0.235 (0.143) | 0.0877 (0.0563) |
| Contact Rate, Funeral ($\beta_F$) | 0.465 (0.287) | 0.283 (0.208) |
| Time from Infection to Hospitalization ($t_H$) | 4.49 (1.44) days | 4.63 (1.43) days |
| Time from Hospitalization to Death ($t_{HD}$) | 3.51 (1.44) days | 3.51 (1.43) days |
| Time from Hospitalization to Recovery ($t_{HR}$) | 5.51 (1.44) days | 5.51 (1.43) days |
| Probability a Case is Hospitalized ($\theta$) | 0.248 (0.142) | 0.233 (0.145) |

Table 3: Calibrated parameters for Ebola epidemic in Liberia. Posterior mean and standard deviation (in parentheses) are listed for pre-intervention and post-intervention calibrations.

Calibration results are shown in Table 3. By observing the posterior mean of the two calibrations, we conclude that our calibration reasonably predicts decreased transmission rates ($\beta_I$, $\beta_H$, $\beta_F$) post-intervention. See Figure 3 for the differences of these parameters; the step function pictured is used when running the systems model. The parameters for time until hospitalization ($\gamma_H$) and the probability a case hospitalized ($\theta$) were calibrated to have the same approximate value pre- and post-intervention. This may be reasonable if, for

example, the hospital capacity insufficient to handle the increasing number of cases. It also tells shows that the system dynamics are more sensitive to the changes in $\beta_I$, $\beta_H$, $\beta_F$ compared to the changes in $\gamma_H$, $\theta$.

We validated our calibration in Figure 4, which shows a good fit between the used cumulative death data and the systems model using the calculated parameter means. This figure, shows a comparison between the proposed model and World Health Organization reported data, the results of our model pre and post intervention and the forecast for the coming months, predicting that after the system reaches an equilibrium, the proportion of deaths in Liberia product of the EVD would be 5.07% approximately.

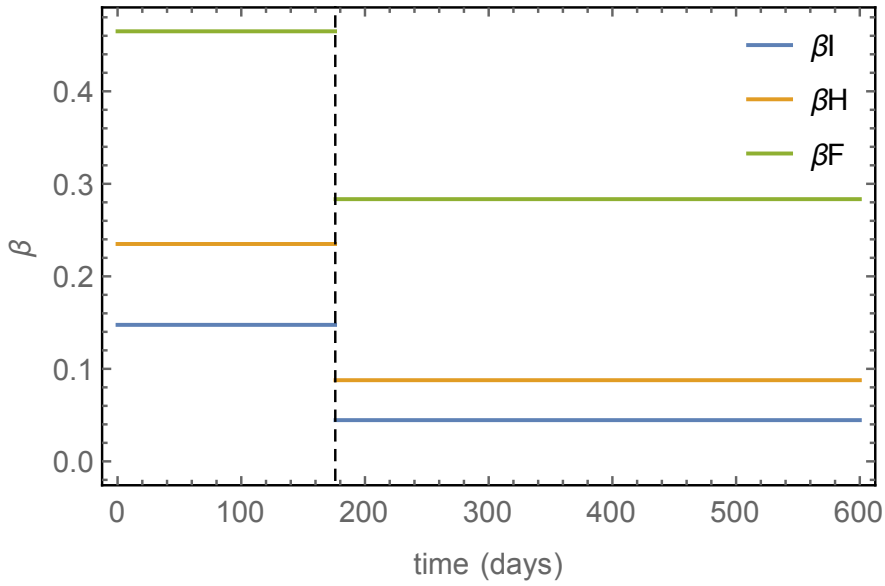


Figure 3: $\beta$ step function

### 3.3 Simulation

Insight Maker is a powerful online tool used to model and simulate complex systems. It utilizes different approaches, such as System Dynamics, Agent-Based Modeling and imperative programming. Insight Maker permits construction of a graphical model to forecast the system response [5]. We used the InsightMaker platform to prototype our model and simulate stepping forward through time. More details about the platform and its functionality can be found in Fortmann-Roe's review. The platform uses two numerical solvers to approximate solutions of the system of differential equations; fourth-order Runge-Kutta method [5].

The compartment S was initialized with a value of 999999, and the compartment I with 1, meaning that there is one infected individual per every million individuals; the rest of the compartments were set to zero as an initial condition. The flows between the compartments are given in the equations and all the other parameters were initialized as shown in Tables 1 and 3. As mention at the beginning of the section, the parameters were calibrated in two stages, before and after the international intervention. According with the time frame proposed, the change in the parameters was also implemented on Insight Maker. The links to the online models can be found on [15] and [16].

After modeling the system with the parameters before the intervention, it can be observed in Figure 5 how the total population decreases to 46.46% if there is no intervention and the each of the parameters continue to be the same. The number of susceptible individuals decays exponentially, converging to 7% of the population, while exposed, infected, hospitalized and funeral comparments converges to zero; finally, after the system stabilizes, the final proportion of deaths would be 53.53%.

As mentioned before, five parameters were calibrated for the second stage of the Ebola outbreak, namely, community contact rate ($\beta_I$), hospital contact rate ($\beta_H$), funeral contact rate ($\beta_F$), time until hospitalization ($\gamma_H$) and probability a case is hospitalized ($\theta$). Figure 6 focuses on E, I, R, H , F and D compartments, showing that the international intervention causes a dramatic change in the behavior of such compartments,

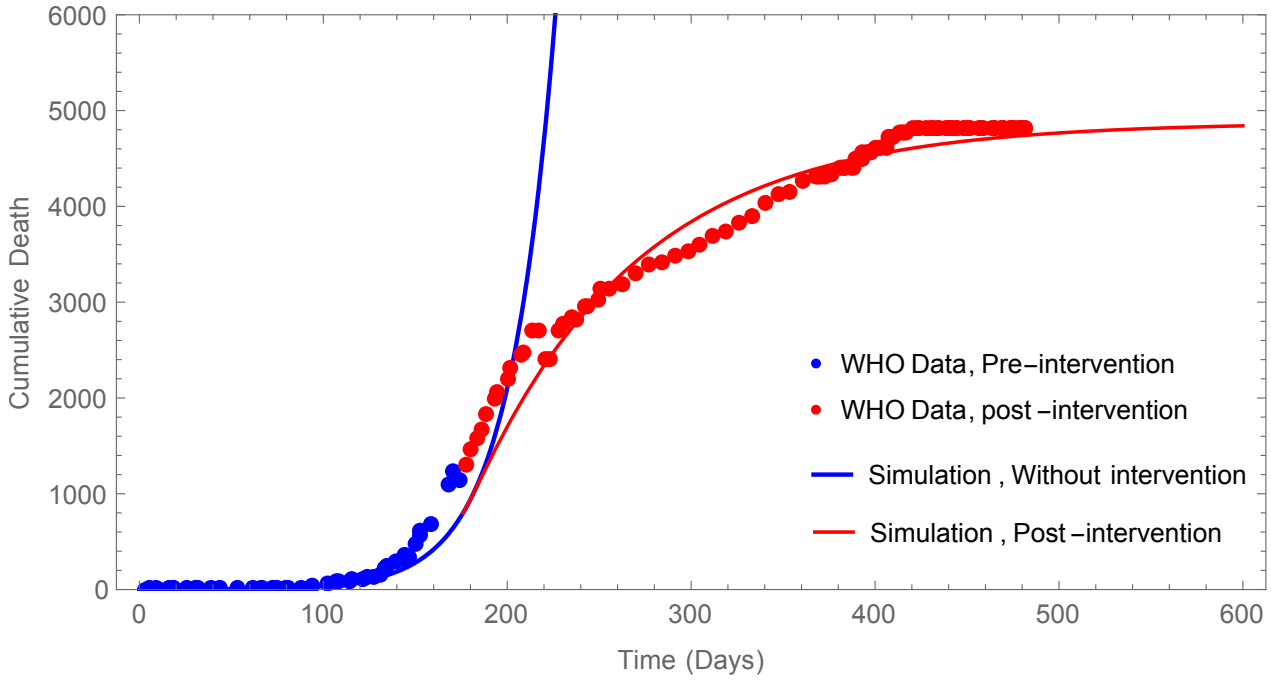


Figure 4: Validation of calibration. Dots represent cumulative death data and the lines represent simulation based on mean posterior parameters. (Blue) - pre intervention and (red) - post intervention.

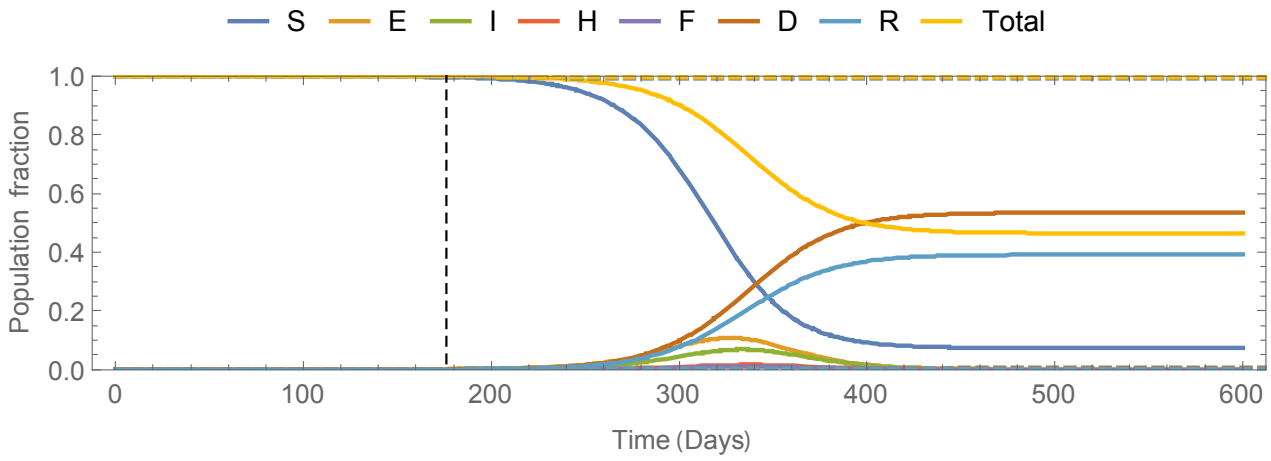


Figure 5: Simulation results using the parameters of the first stage (Mar 2014 to Sept 2014) and assuming no intervention

meaning that the virus was controlled.

Figure 7 shows another visualization of our simulation on 2 dimensional space of $S + R$ vs. $D$. By watching the phase portrait in the figure, we can see that the fraction of survived population after outbreak $S+R$ converges to 46% and dead people $D$ converges to 54% without intervention. However, with intervention on 176th day, the $S + R$ and $D$ converge to 99.5% and $0.487 \times 10^{-3}$%, respectively. The significant effect of intervention observed here can be analyzed by the basic reproduction number ($R_0$). $R_0$ is a indicator to tell if the infection will spread (if $R_0 > 1$) or die out (if $R_0 < 1$) eventually in the population. Evaluated Based on (reference), $R_0$ is $1.99(> 1)$ before intervention. However, it has been changed with after intervention to $0.786(< 1)$.

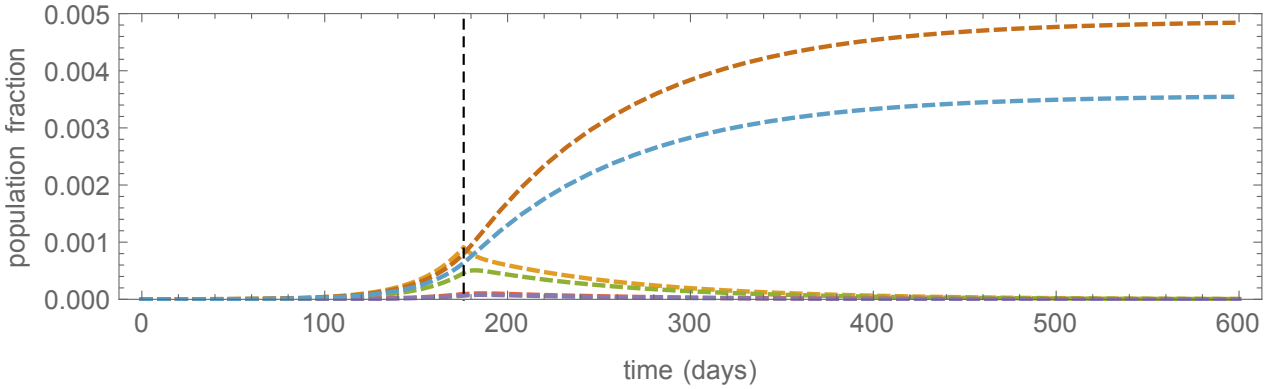


Figure 6: Parameters of the second stage ( Sept 2014 to July 2015).

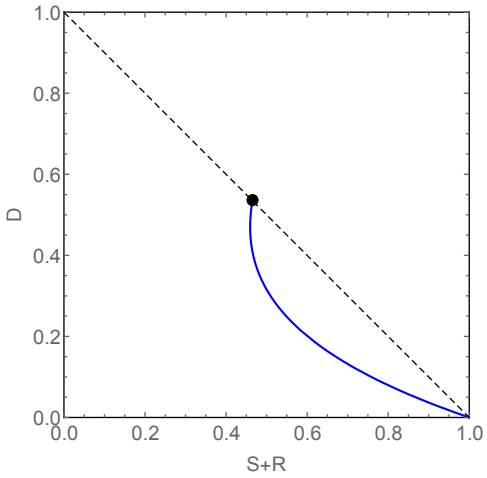


(a) Full scale

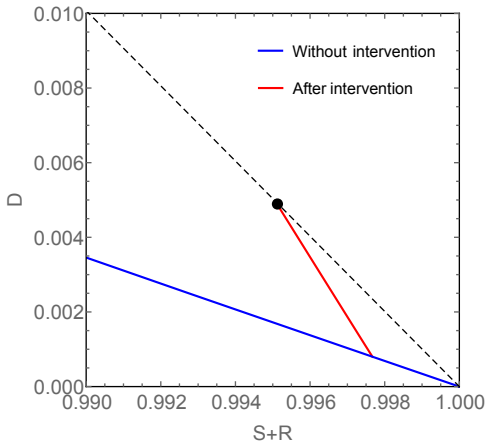


(b) Rescaled plot of (a) to enlarge right bottom corner

Figure 7: Projection of phase portrait to (Susceptible + Recovered, Dead) space. (Blue) - without intervention, (Red) - with intervention, (Dots) - where the phase converges (equilibrium)

# 4 Agent-Based Dynamics

The next model we consider is an agent-based model. Each individual in the population can be in one of 7 states discussed above: susceptible, exposed, infected, hospitalized, funeral, recovered or dead. The flow between two states is a probability of transition from one state to another for a typical individual. We represent our model in Figure 8. In each time step a typical individual who is susceptible can either transition to an exposed state with probability $p_{SE}$ or stay susceptible with probability $p_{SS}$. An individual in the exposed state transitions to infected with probability $p_{EI}$ and stays exposed with probability $p_{EE}$. An individual who is infected can stay infected, recover, go to a hospital, or die and transition to the funeral state with probabilities $p_{II}$, $p_{IR}$, $p_{IH}$ and $p_{IF}$, respectively. Recovery is considered a terminal state so individuals in this state stay in it for the remainder of the simulation. Hospitalized individuals may stay hospitalized, transition to recovered or funeral with probabilities $p_{HH}$, $p_{HR}$ and $p_{HF}$. We assume that the individual who dies from Ebola remains infectious through the duration of the entire burial ceremony and no precautions are taken against disease transmission. Safely buried individuals are considered noninfectious and remain in this state.

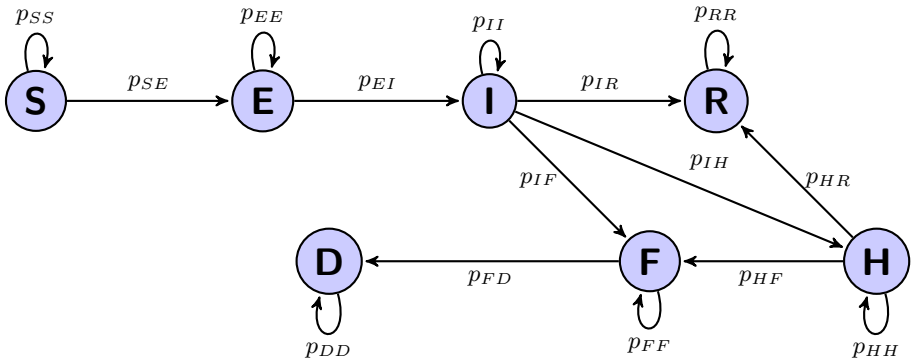


Figure 8: Spread of the disease: Agent-based model. Each node represents a typical individual's state. An individual can transition to a state to which he is connected by a directed arc with a probability specified on an arc.

We let $N$ be the total number of individuals in a population, $N_I$ be the total number of individuals in the infected state, $N_H$ be the total number of individuals in the hospitalized state and $N_F$ be the total number of individuals in the funeral state. We define and present numeric values of individual's probability of transition for each state in Table 4. In calculating the probabilities we used parameters found in Table 1 and Table 3.

## 4.1 Simulation

We consider a population of size 1000 with 999 individuals starting in a susceptible state and 1 individual in the exposed state. This means that the scale of our probabilistic model is different from the scale of the system-based model so that there is not necessarily a direct correspondence between the results. Numeric probabilities of an individual transitioning from each state are recorded in Table 4. We run one hundred Monte Carlo simulations and average the results to estimate an outcome of the disease. We define an outbreak as an event in which 2% of the population or more contracts the disease. If only one individual is exposed to the disease in a population of 1000, there is about 30% chance that the outbreak does not happen (27/100 trials). However, once the cumulative proportion of the exposed individuals reaches 1%, the virus affects more than 90% of the population. A histogram for simulation outcomes is depicted in Figure 9.

We note that the simulations reach their stationary state before $t = 300$. We plot the result of 100 simulations in Figure 10. In a number of simulations, no outbreak of Ebola is observed. However there are many cases which show catastrophic disease. In the disastrous case, on average, 93% of people get the disease and 50% of people die from it.

If there is no outbreak, the infected agent may or may not infect another agent in the population. However, most people remain in the susceptible state because the infected individual recovers or dies before infecting

| Parameter | Definition | Liberia Before Intervention (Mar 2014 to Sept 2014) | Liberia After Intervention (Sept 2014 to Jul 2015) |
|---|---|---|---|
| $p_{SE}$ | $\beta_I N_I/N + \beta_H N_H/N + \beta_F N_F/N$ | Dynamic | Dynamic |
| $p_{SS}$ | $1 - p_{SE}$ | Dynamic | Dynamic |
| $p_{EE}$ | $1 - 1/t_P$ | 0.9091 | 0.9091 |
| $p_{EI}$ | $1/t_P$ | 0.0909 | 0.0909 |
| $p_{II}$ | $1/t_I$ | 0.1 | 0.1 |
| $p_{IH}$ | $1/t_H$ | 0.2227 | 0.2160 |
| $p_{IF}$ | $1/t_D$ | 0.125 | 0.125 |
| $p_{IR}$ | $1 - p_{II} - p_{IH} - p_{IF}$ | 0.5523 | 0.559 |
| $p_{HF}$ | $1/t_{DH}$ | 0.2849 | 0.2849 |
| $p_{HR}$ | $1/t_{IH}$ | 0.1815 | 0.1815 |
| $p_{HH}$ | $1 - p_{HF} - p_{HR}$ | 0.5336 | 0.5336 |
| $p_{FF}$ | $1/t_F$ | 0.5 | 0.5 |
| $p_{FD}$ | $1 - p_{FF}$ | 0.5 | 0.5 |
| $p_{RR}$ | 1 | 1 | 1 |
| $p_{DD}$ | 1 | 1 | 1 |

Table 4: Agent-based Model Parameters for Ebola Epidemic in Liberia with and without the International Intervention.

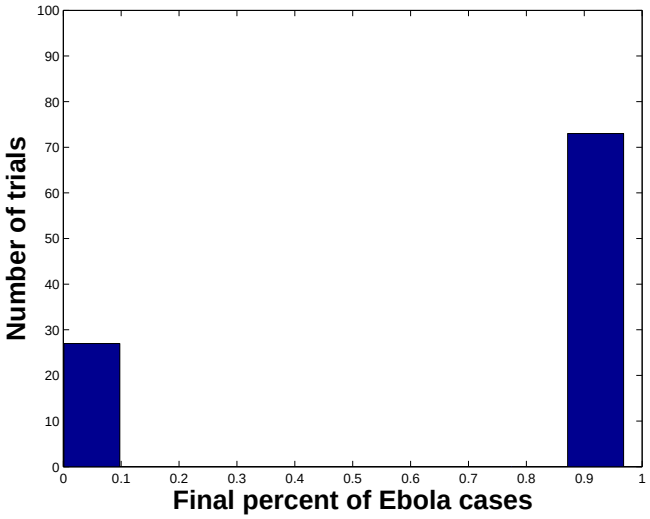


Figure 9: Histogram showing the outcome of 100 simulations: 27 trials experience no outbreak and 73 trials do.

enough people to cause an outbreak. The proportion of the population that gets Ebola is low, so all seven states stay relatively constant over time.

On the other hand, if the infected agent contacts many people while infected (I), hospitalized (H), or in a funeral state (F) before transitioning to state D or R, there is a an outbreak of the disease. A typical outbreak is depicted in Figure 11. The proportion of agents who contract the disease grows exponentially until $t = 125$. That is also the time at which the proportion of the population in states I, H, and F is the highest. After that, the population does not have enough susceptible agents to spread the disease causing the proportion of exposed agents to decrease. The proportion of agents in I, H, and F decreases as well. Around $t = 180$ the proportion of the population is states I, H, and F is zero; the proportion of the population in state S does not decrease, i.e. no agents get Ebola. At this point, every agent remains in S, R or D and an equilibrium

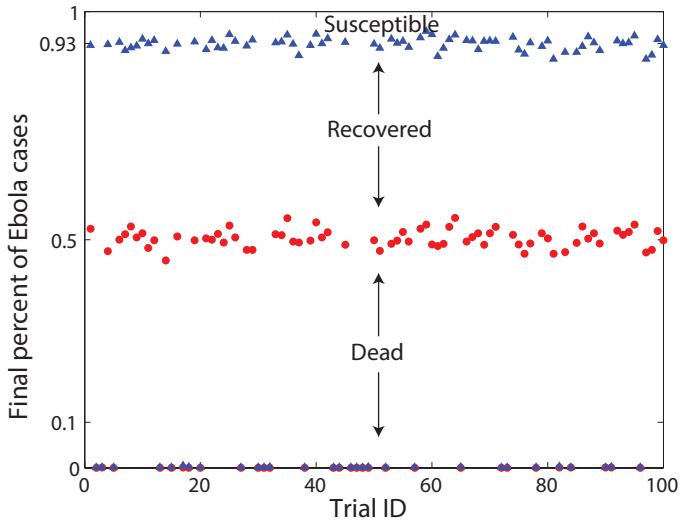


Figure 10: Scatter plot showing the proportion of population that contracts the disease (blue) and the proportion of the population that dies due to the disease (red) for a population size 1000.

is reached (stable fixed point). As we showed before, on average, 7% of agents stay in state S, 43% of agents stay in R, and 50% of agents would be in D.

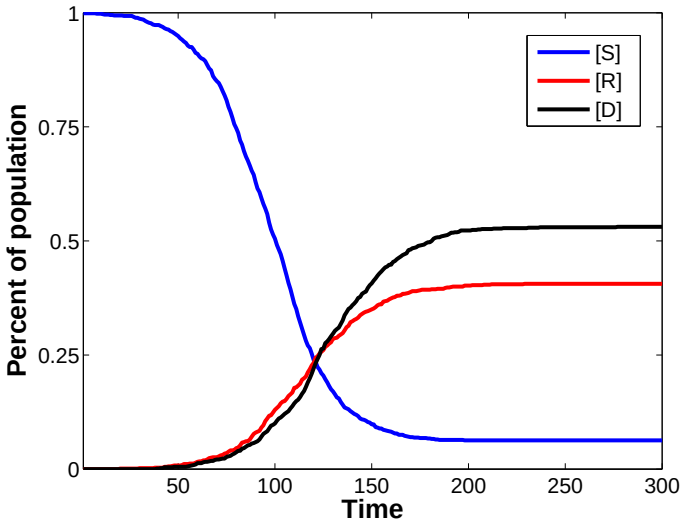


Figure 11: One realization of an outbreak.

We plot a phase portrait for the proportion of agents who never got infected and are in S versus the proportion of agents who contracted the disease (both D and R) as time progresses. On the horizontal axis, we put the ratio of S to the total population and on the vertical axis - the ratio of D plus R to the total population. When $t = 0$, one agent is in state E and 99.9% of agents are in S. All other states contain no agents. About 30% of the time, there is no outbreak. In such case, only few people get Ebola. As time goes by there are only few transitions between states and a stationary point is reached within a few time steps. However, if there is an outbreak, the trajectory gradually moves to its equilibrium state. On

average, the equilibrium occurs at $(S, R+D) = (0.07, 0.93)$. We conduct one hundred experiments and plot their trajectories on the same graph, presented in Figure 12. Because the total proportion of people in the population is one, the equilibria in different experiments lie on the $x + y = 1$ line. The system starts at $(S, R+D) = (0.999, 0)$, a point that is close to this line. During the course of the outbreak, the phase portrait falls below the black line because a portion of the population are in the transient states: E, I, H and F.

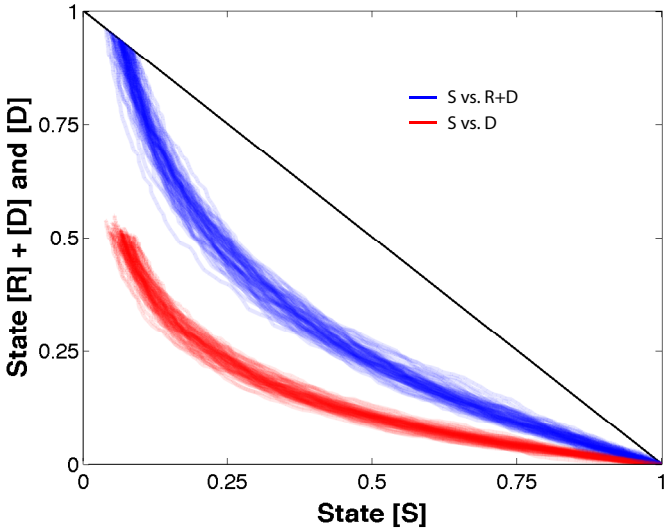


Figure 12: Phase portrait: proportion of the population who are in susceptible state versus proportion of the population who contracted Ebola (blue) or are dead because of it (red) for different uncertainty realizations.

As in the system dynamics approach, we perform an intervention in the agent-based model. Because the scale in the two models is different, we implement the intervention step if we see a total of 1% of agents contracting the disease. At the beginning of intervention, we change the three $\beta$s, representing the different contact rates. Our results, presented in Table 5, show that if we start the intervention at 1% of population having Ebola, 4% of agents get the disease, 2% of agents recover and 2% of agents die. This is a significant improvement over the disastrous predicted outcome of an outbreak without an intervention.

| | No Intervention | Intervention |
|---|---|---|
| Final $S$ | 7% | 96% |
| Final $R$ | 43% | 2% |
| Final $D$ | 50% | 2% |

Table 5: Percent of the total population in different states with and without intervention.

We examine the effect of the population size on the outcome of the agent-based model. Besides the baseline case of $N = 1000$, we set the total population to be $N = 100$ and 5000. The results show that an increase in population size decreases the standard deviation of the quantities S, D and R, but the relative averages remain the same. As the population size increases stochastic variation decreases and the system becomes more predictable.

We also examine the probability of outbreak occurring based on the population size. The results are presented in Figure 13. As population size increases, the probability of outbreak occurring decreases but never gets below around 70 %.

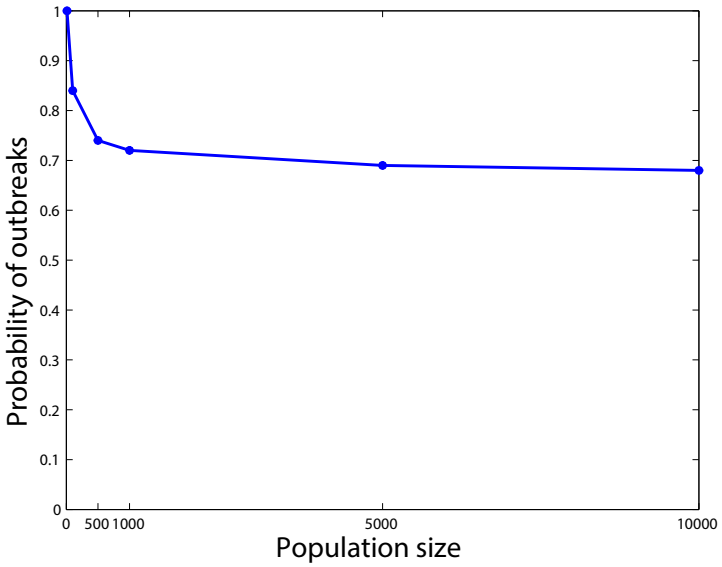


Figure 13: Probability of an outbreak as population size varies.

# 5 Spatial Agent-Based Dynamics

We next look at an agent-based model where agents are allowed to move within and between cities. Incorporating spatial movement requires making additional assumptions about the map on which movement is allowed and the movement of individuals. The model is coded in `Python` and propagates the infection and spatial information in discrete days.

## 5.1 Spatial Assumptions

We restrict the space (on which cities and individuals are located) to a specified width and height and generate cities randomly within the space with specified relative density and population variance from the city center. For example, a model may have one city with variance 30 and density 0.9 and a village with variance 5 and density 0.1. Locations of individuals and cities are real numbers. We also create a grid, which partitions the individuals based on their location and is used to determine the closest neighbors for community infection and funeral attendance. A family is assumed to have $n_{fam}$ members all of which live in the same exact location. Upon initialization (and later travel), families are place based on the specified city densities, normally distributed around the city's center location using the city's variance. We define an individual's *home* as their initial location.

An individual is *movable* if he is susceptible, exposed, or recovered. All other individuals remain stationary. Movable individuals travel each timestep with probability $p_{trav}$. If they are away from home, they will travel home with probability $p_{home}$. Otherwise, they will travel locally (within their current city or village) or non-locally (to another city) based on the density of their current city. It is assumed that when an individual is in a city with higher density they are less likely to leave. If individual $i$'s current city density (percentage of the total population) is $d(i)$, then the non-local travel probability is $(1 - d(i))/2$. In the local and non-local travel, the individual is again normally distributed around that city's center.

## 5.2 Agent Behavior

The model uses the same states as the previous models, but some of the transitions and probabilities have been modified. Specifically, hospitalized individuals are assumed to be quarantined, and thus no longer infect others or have funerals. Instead, hospitalized individuals move straight to the dead state upon death. See Figure

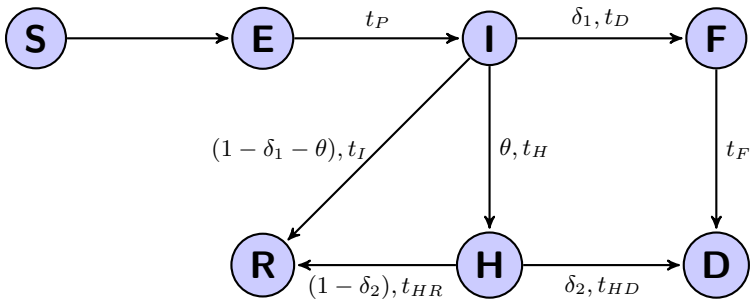


Figure 14: Available states for individuals and the transitions between them. Probabilistic transitions and timeouts between states are listed along the transitions. If both are present, once it is decided that the individual will transition, the timeout is calculated and counted down. The transition from susceptible to exposed is based on the surrounding infected individuals using transmission probabilities $\eta_f, \eta_c, \eta_F$.

8 vs Figure 14 for a comparison between the two agent-based models. Figure 14 denotes the probabilistic and timeout transitions between states. We define a *timeout* to be an integer number of days to wait before transitioning to another state, either uniformly randomly generated between two integers or equal to a specified constant. Whenever a range of integers is listed, the integer used in simulation is uniformly drawn from that range.

The spatial movement and transitions between states is dependent on the individual's current state. Following are a description of the behavior of each type of individual.

**Susceptible** individuals travel randomly and may only transition to the exposed state.

**Exposed** individuals may also travel randomly. Upon initial transition, they generate a timeout of $t_P$ days until they will transition to the infected state.

**Infected** individuals are assumed to be too sick to travel. Upon initial transition, it is decided whether they will go to the hospital (with probability $\theta$, generating a timeout of $t_H$ until transitioning to hospitalization), die and be buried at a funeral (with probability $\delta_1$, generating a timeout of $t_D$ until transitioning to the funeralized state), or recover (generating a timeout of $t_I$ until transitioning to the recovered state). While in the infected state, the individual infects people in the surrounding grid each with probability $\eta_f$ if they are a family member or $\eta_c$ if they are a typical community member. See Figure 15 for a visualization.

**Hospitalized** individuals are quarantined and no longer infect anyone. Upon initial transition, it is decided whether they will die in the hospital (with probability $\delta_2$, generating a timeout of $t_{HD}$ until death) or recover (generating a timeout of $t_{HR}$ until recovery). Because they are quarantined, traditional funerals with high infection rates are not held upon death.

**Funeralized** individuals spend $t_F$ days in the funeralized state before transitioning to the dead state, but only infect people on the initial entrance to the funeralized state. Upon initial transition, the individual and all of their movable relatives return home. All susceptible people in the individual's home grid cell who were also in that grid cell at initialization (family and initial neighbors not currently away) are then infected with probability $\eta_F$. See Figure 15.

**Recovered** individuals do not affect the model but can continue traveling.

**Dead** individuals remain stationary and do not affect the model.

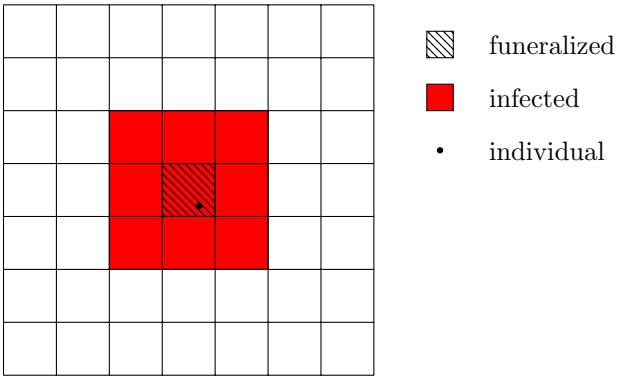


Figure 15: Grid cells affected by funeralized and infected individuals. Infected individuals may infect other family or community members in the red region. Funeralized individuals may infect others in the shaded cell – family members, who all return home for the funeral or community members who were originally located in that cell and are considered neighbors.

### 5.3 Parameters

Parameter values used in the simulations are listed in Table 6. Other parameters specific to the modeling procedure include map width (70) and height (70), number of cities (3), city densities $(80\%, 10\%, 10\%)$ and variance $(20, 5, 5)$, number of timesteps until termination (500), and population size (1000).

| Parameter | Variable | Value |
|---|---|---|
| Travel probability | $p_{trav}$ | 0.2 |
| Travel, home probability | $p_{home}$ | 0.5 |
| Travel, non-locally probability | $p_{nonloc}$ | $(1 -$ current city density$)/2$ |
| Family size | $n_{fam}$ | 3-6 |
| Family infection probability per day | $\eta_f$ | 0.1 |
| Community infection probability per day | $\eta_c$ | 0.006 |
| Funeral infection probability per day | $\eta_F$ | 0.2 |
| $^\star$Funeral length | $t_F$ | 2 |
| $^\star$Incubation time | $t_P$ | 11 days |
| $^\star$Infected mortality | $\delta_1$ | 0.5 |
| $^\star$Time from infection to death | $t_D$ | 7-9 days |
| $^\star$Time from infection to recovery | $t_I$ | 10 days |
| $^\star$Hospitalization probability | $\theta$ | 0.248 |
| $^\star$Time until hospitalization | $t_H$ | 3-6 days |
| $^\star$Hospital death probability | $\delta_2$ | 0.5 |
| $^\star$Time from hospitalization to death | $t_{HD}$ | 3-4 days |
| $^\star$Time from hospitalization to recovery | $t_{HR}$ | 5-6 days |

Table 6: Parameter values used in the model. Values marked with $^\star$ (in the third group) are based on data from Tables 1 and 3. Values from the second group were chosen so that the $R_0$ value calculated from the spread of infections in the first 30 days was approximately 1.5-2. Travel values and family size in the first group were chosen heuristically.

Although the values may not precisely match those from the Ebola outbreaks, they still provide some insight into the spread of a disease through a spatial model.

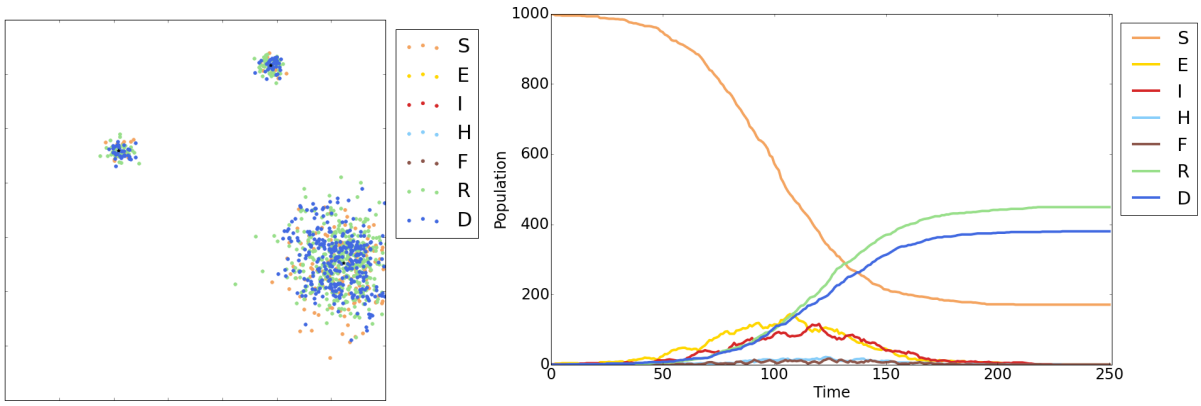


(a) Map of final states

(b) Time series of simulation.

Figure 16: Example simulation plots with one city (density 0.8) and two villages (each with density 0.1). The map on the left corresponds to the time series plot on the right.

### 5.4 Results

We initialize the model with one infected individual who does not go to a hospital and does not recover. In Figure 16, we show plots of an example simulation of the final individuals (location and state) and of the time series counting how many individuals are in each state at each step in time. Figure 17 shows 200 time series of the susceptible, recovered, and dead state count, with the average of the simulations with outbreaks. The spread of the instances is similar to that in Figure ? from the non-spatial agent-based model. Because the spatial system is not well-mixed, we see that less individuals contract the disease and are able to remain in the susceptible class. The number of people in the recovered and dead classes are the same on average because once an individual contracts the disease, they have a 50% chance to recover and a 50% chance to die (see Table 6).

As can be seen in Figure 19, about 80% of the simulations result in an outbreak, which is defined as more than 2% of the population contracting the disease as in Section 4. Unlike the model in Section 4, the outbreaks can be less severe. When an outbreak occurs it may not infect the entire population (see Figure 9) – this is expected, as that model assumes a well-mixed population in the infection dynamics, whereas this spatial model allows individuals to escape the disease through movement to non-infected areas.

Because this model uses families, we are able to differentiate between the infections resulting from family, community, and funeral contact. If a family member contacts the deceased at a funeral we consider the transmission one by funeral contact. We show the data from 25 simulations in Figure 18. Out of 200 trials, the disease spread on average 17% through family contact, 70% through community contact, and 13% through funeral contact. These rates are highly reliant on the different infection probabilities $(\eta_f, \eta_c, \eta_F)$, which were chosen so that the combination gave a reasonable $R_0$ value; however, increasing one infection probability and decreasing another could give the same $R_0$ value and very different percentages. With the given parameters, however, transmission between community members accounts for the highest proportion of disease contraction. Funeral and family contact both still account for a significant portion of the infections, which suggests that decreasing the contact with the deceased during funerals may significantly decrease the number of infections.

## 6 Summary and Future Work

In this paper we examined time series data of the number of Ebola cases and deaths in Liberia during the 2014-2015 outbreak. Through a system dynamics approach, we showed that intervention can have a significant impact on the spread of the disease. A change in model parameters, caused by international intervention, decreased Ebola's reproductive number from 1.99 to 0.787. Because system dynamics is a deterministic approach, we also looked at an agent-based variation of the model, which allows us to observe realizations with and without outbreaks (if the infected individual dies, the disease is not spread). Through different

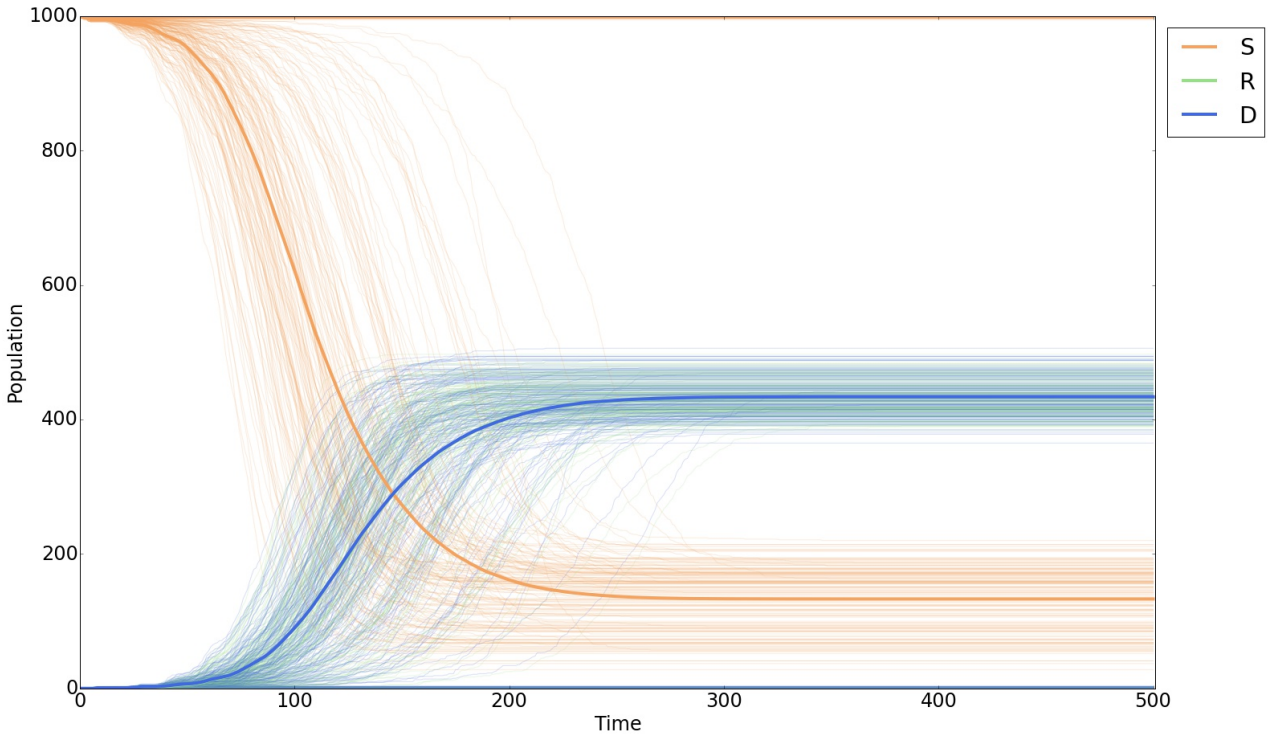


Figure 17: Time series graphs of the number of individuals in the susceptible, recovered, and dead states of 200 simulations. The averaged values of simulations in which an outbreak occurred are the bold curves.

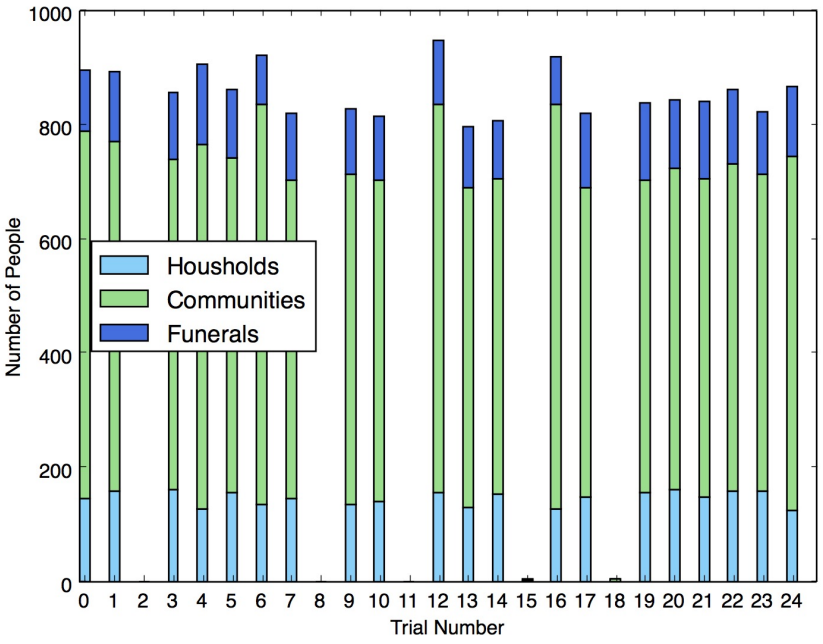


Figure 18: The number of infected individuals in 25 trials based on how the disease was transmitted: through family, community, or funeral interactions. These simulations used a population size of 1000 and ran for 500 timesteps.

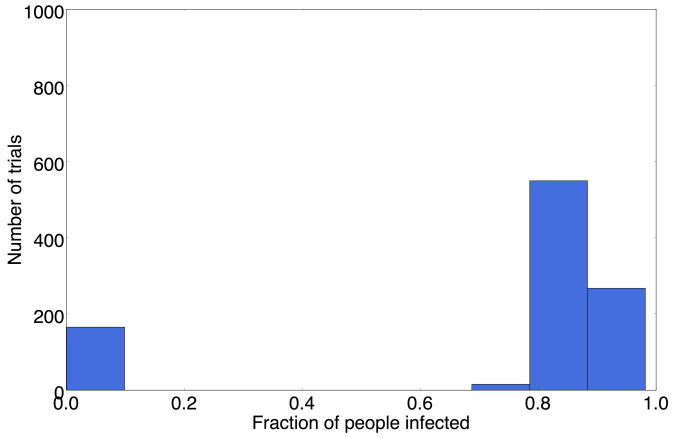


Figure 19: A histogram showing the fraction of people infected in each trial, run with 1000 trials. About 20% of trials do not exhibit an outbreak.

realizations, we saw that in 70% of the instances Ebola would spread to more than 2% of the population with severe consequences: half of the population dies. Through the probabilistic model we also studied the effect of intervention. If the intervention is started early, when only 1% of the population is exposed to the disease, only 2% of the population dies. This model assumed that the population is well-mixed, which is unrealistic – for example, in Africa there are many small villages and larger cities, and the spread of a disease can depend highly on the amount of movement of the infected individuals. The recent Ebola outbreak started in one such small village. To take such inhomogeneous densities into account, we then incorporated spatial movement into an agent-based model and allowed for different types of individuals (family vs. community) and local transmission of the infection. In this setting, the outbreaks can be less severe due to the environment not being well-mixed. When tracking how many infections result from different types of contact, the spread between community members accounts for the highest proportion of transmission. The transmission during funerals is still significant, however, and reducing the common practices of touching the deceased at a funeral would lower the number of infected individuals.

The system dynamics approach provides the average expected dynamics of an Ebola outbreak and clearly shows the parameter's effects to the model in the system of differential equations. The non-spatial agent-based model gives a probabilistic approach to such average dynamics, allowing Ebola cases to die out and prevent outbreaks. This model is appropriate to use in a well-mixed population. In a population that is not well-mixed or with multiple cities and villages that are spatially disconnected, the spatial agent-based model provides a more flexible model although the parameters interactions are less clear than in the previous two models.

There are several factors one may wish to take into account when analyzing how a virus spreads in a community. We took into account characteristics of the virus itself: incubation period, the rate of recovery, mortality rate and society's cultural perspective on a proper burial ceremony. In the spatial model we also attempted to incorporate frequency and nature of individuals' interactions, and distance and frequency of travel to other villages. Other factors also play a role in the spread of the disease. Having information about the local government and the wealth of the region would help to determine the capacity of response when facing an epidemic, including the quantity and quality of hospitals, their capacity, and the number of health-care professionals as well as their level of expertise. In the moment of a virus outbreak, governments from other countries may intervene to help to control the disease, possibly decreasing the number of infected people and increasing the number of recovered patients, by educating individuals about the virus and its mode of transmission as well as properly handling the deceased family. One realization of the result of such action we saw during 2014-2015 Ebola outbreak in Liberia. Such social parameters could be incorporated into our models.

# References


[1] The World Bank. Liberia. http:http://www.worldbank.org/en/country/liberia/.

[2] Center for Disease Control and Prevention. Ebola virus disease. http://www.cdc.gov/vhf/Ebola/index.html.

[3] Center for Disease Control and Prevention. Ebola virus disease: Previous case counts. http://www.cdc.gov/vhf/Ebola/outbreaks/2014-west-africa/previous-case-counts.html.

[4] Center for Disease Control and Prevention. Outbreaks chronology: Ebola virus disease. http://www.cdc.gov/vhf/Ebola/outbreaks/history/chronology.html.

[5] S. Fortmann-Roe. Insight Maker: A general-purpose tool for web-based modeling & simulation. *Simulation Modeling Practice and Theory*, 47:28–45, 2014.

[6] J. Legrand, R. F. Grais, P. Y. Boelle, A. J. Valleron, and A. Flahault. Understanding the dynamics of Ebola epidemics. *Epidemiology and Infection*, 135:610–621, 2007.

[7] P. E. Lekone and B. F. Finkenstdt. Statistical inference in a stochastic epidemic SEIR model with control intervention: Ebola as a case study. *Biometrics*, 62:1170–1177, 2006.

[8] S. Merler, M. Ajelli, L. Fumanelli, M. F. C. Gomes, A. P. Piontti, L. Rossi, D. L. Chao, I. M. Longini Jr., M. E. Halloran, and A. Vespignani. Spatiotemporal spread of the 2014 outbreak of Ebola virus disease in Liberia and the effectiveness of non-pharmaceutical interventions: a computational modeling analysis. *The Lancet Infectious Diseases Journal*, 15:204–211, 2015.

[9] World Health Organization. Ebola virus disease: Fact sheet n103. http://www.who.int/mediacentre/factsheets/fs103/en/.

[10] World Health Organization. Factors that contributed to undetected spread of the Ebola virus and impeded rapid containment. http://www.who.int/csr/disease/Ebola/one-year-report/factors/en/.

[11] C. Poletto, M.F. Gomez, A. Pastore y Piontti, L. Rossil, D.L.Chao, I.M. Longini, M.E. Halloran, V. Colizza, and A. Vespignani. Assessing the impact of travel restrictions on international spread of the 2014 West African Ebola epidemic. *Eurosurveillance*, 19.

[12] C. M. Rivers, E.T. Lofgren, M. Marathe, S. Eubank, and B. I. Lewis. Modeling the impact of interventions on an epidemic of Ebola in Sierra Leone and Liberia. *PLOS Currents Outbreaks*, 2014.

[13] C. Siettos, C. Anastassopoulou, L. Russo, C. Grigoras, and E. Mylonakis. Modeling the 2014 Ebola virus epidemic agent-based simulations, temporal analysis and future predictions for Liberia and Sierra Leone. *PLOS Currents Outbreaks*, 2015.

[14] G. Webb, C. Browne, X. Huo, O. Seydi, M. Seydi, and P. Magal. A model of the 2014 Ebola epidemic in West Africa with contact tracing. *PLOS Currents Outbreaks*, 2015.

[15] N. Yoon and D. Velez-Rendon. Liberia: Modeling Ebola virus disease after international intervention. https://insightmaker.com/insight/34971/Ebola-Liberia-Before-After-Intervention.

[16] N. Yoon and D. Velez-Rendon. Liberia: Modeling Ebola virus disease before international intervention. https://insightmaker.com/insight/34914/Ebola-Liberia.